Correcting Beam Hardening and Visibility Hardening Artifacts in Dark-field CT

LSU
Department of Physics & Astronomy

Hunter C. Meyer[1,*], Joyoni Dey[1]
[1] Department of Physics and Astronomy, Louisiana State University
* Currently: Department of Radiology, University of Colorado Anschutz School of Medicine

MEDICAL PHYSICS COMMUNITY
INSPIRATION INNOVATION IMPACT
2026 JULY 19–22 VANCOUVER, BC
JOINT AAPM | COMP MEETING

Introduction

Attenuation

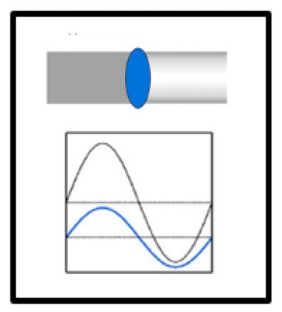

Phase Shift

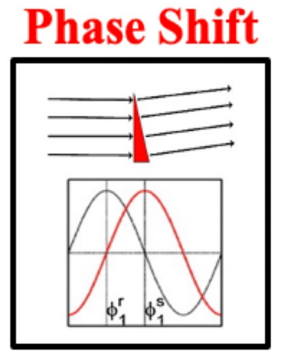

SAS

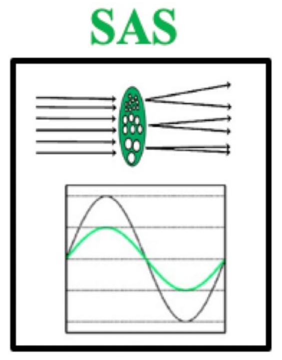

Grating Interferometry

- Diffraction grating: Produces a periodic interference pattern (known as fringes)
- Patient distorts the fringe pattern
- Measure the fringe distortions to produce three unique images

Unique Image Contrast

- X-ray absorption decreases the average value of the fringe pattern (traditional X-ray)
- X-ray refraction shifts the fringe pattern (phase shift)
- X-ray scatter blurs the fringe pattern
  - Reduces the fringe visibility

Produce Three Images

- Attenuation: X-ray absorption
  - Same as a traditional X-ray image
- Differential-phase contrast: X-ray refraction
- Dark-field: Small Angle X-ray scatter (SAS)

Background and Methods

Beam Hardening in Traditional X-ray Imaging

- The average X-ray energy increases with penetration
- Results in shadows and cupping artifacts

Polychromatic Intensity

- $I(E) = a_0(E) + a_1(E)\sin\phi(E)$
- $\bar{I} = \int I(E)S(E)dE$

Polychromatic Transmission and Visibility

- $\bar{T} = \int T(E)S(E)dE$
- The visibility spectrum, $V(E) = \frac{a_1(E)}{a_0(E)}$, is determined by diffractive effects
- Polychromatic visibility incorporates both transmission and scatter effects
  - $\bar{V} = \int T(E)D(E)V(E)S(E)dE$

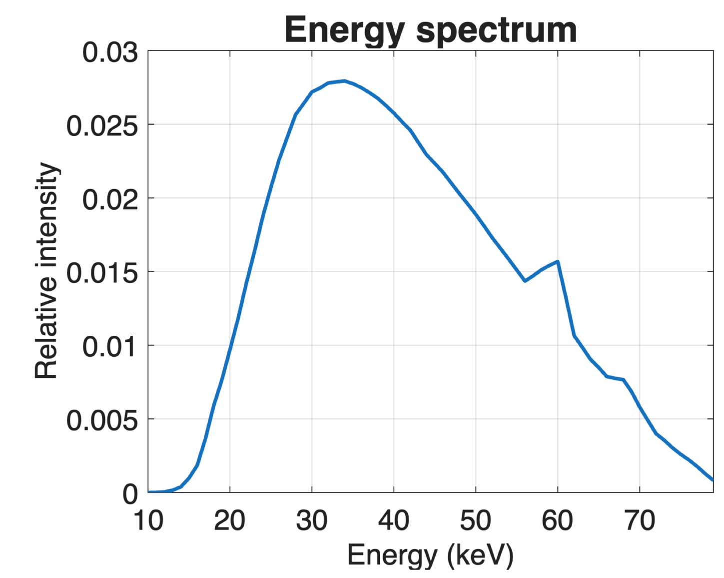

Source: *TASMIP Calculator*[5]

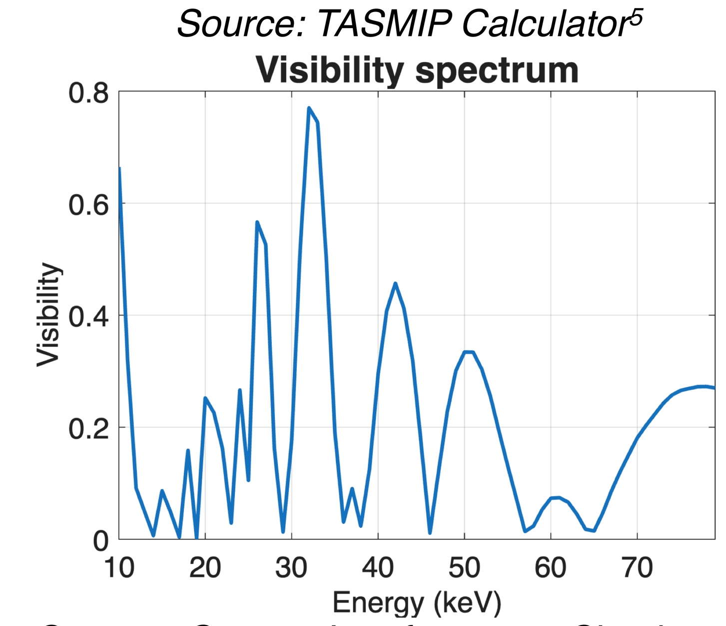

Source: Custom Interferometry Simulator

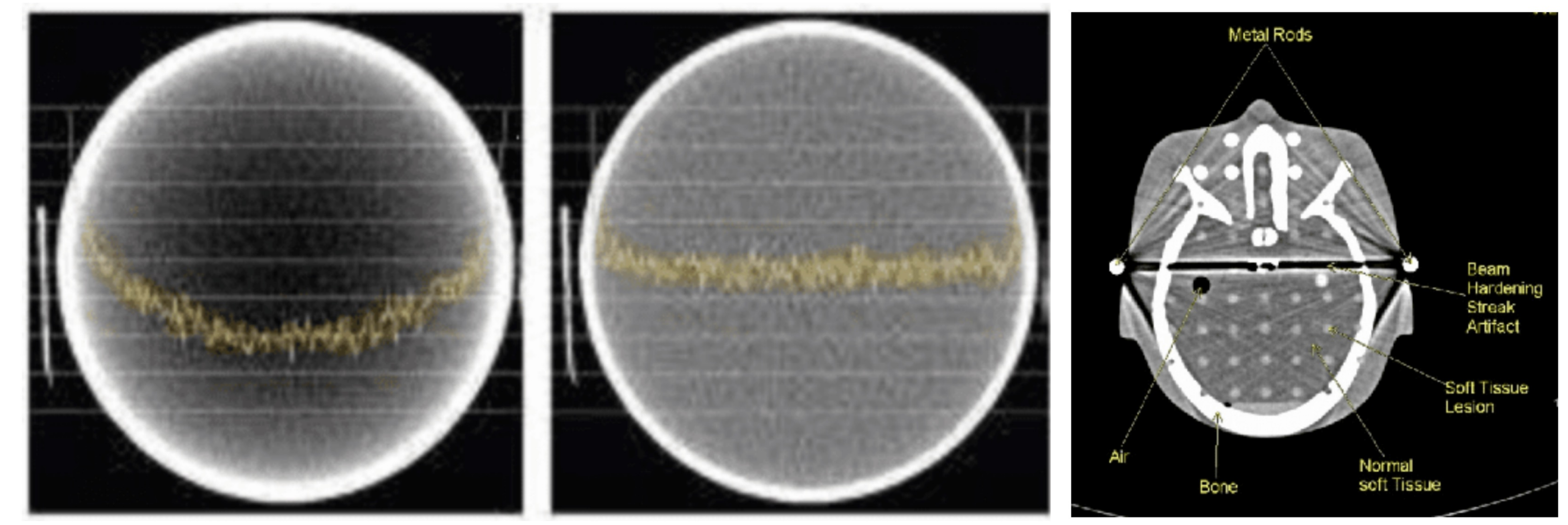

Beam Hardening Artifacts in traditional CT[6]. Left: cupping, middle: corrected, right: streaking.

Correction Strategy

- Incorporate a polychromatic model of $D(E) = e^{-\epsilon t}$
  - Power-law Distribution[7], $\epsilon(E) \propto \frac{1}{E^{-p}}, p \in [2,4]$
- Optimization forms a pseudo-monochromatic image (requires thickness maps, t_m, determined from attenuation CT

$$\text{Optimization Objective: } Q(u,v,\theta) = \sum_m \epsilon_m(E_{ref},u,v,\theta)t_m(u,v,\theta)$$

$$\hat{Q}(u,v,\theta) = \frac{\text{zero}}{Q(u,v,\theta)}\left(\int_E Q(u,v,\theta)\left(\frac{E}{E_{ref}}\right)^{-p} T(E,u,v,\theta)dE - \bar{V}_1^s(u,v,\theta)\right)$$

Clinical Applications of X-ray Interferometry

Lung Imaging

- Potential to improve sensitivity and specificity for lung cancer screening and diagnosis
- Improved imaging of other lung diseases, such as emphysema and fibrosis [2]
- Potential to replace certain indications for CT with radiographic interferometry
- Dark-field Computed Tomography

Breast Imaging

- Dark-field imaging to improve the detection and classification of microcalcifications [3]
- Differential-phase contrast images may improve detection of neoplasms, such as multifocal tumors [4]

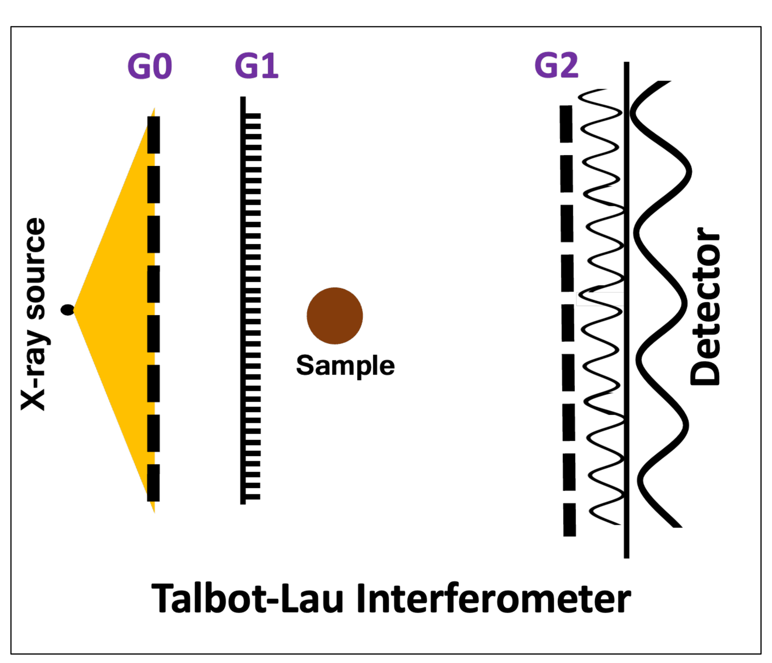

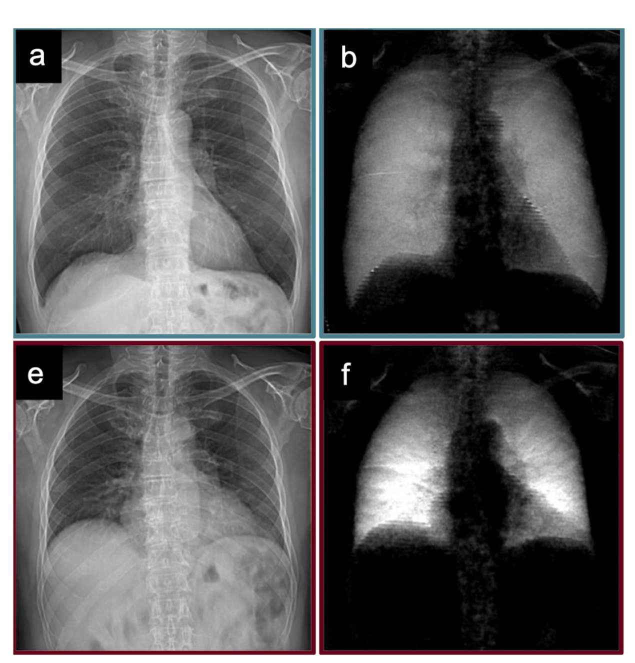

Left: Schematic of the Talbot-Lau Interferometer. Right: Comparison of attenuation (left) and dark-field (right) images for patients at full inhale (top) and full exhale (bottom), source: Urban et al [8]

Results

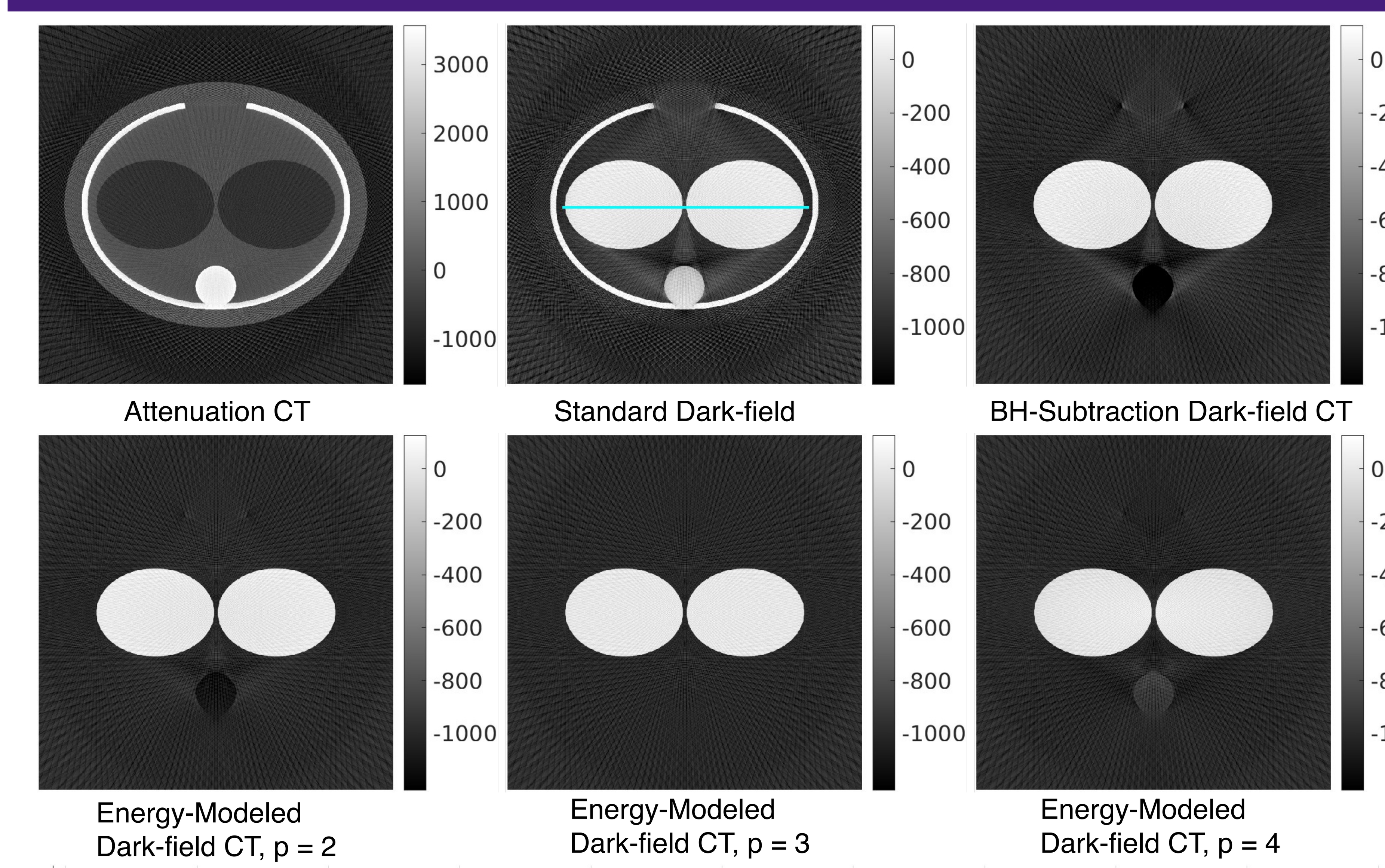

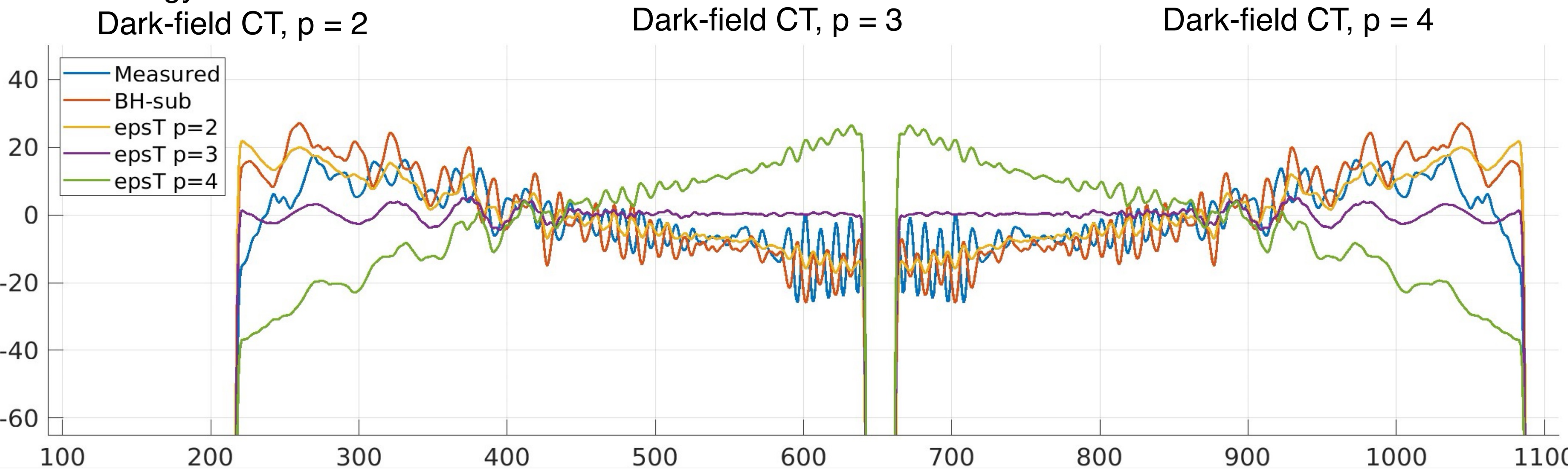

Demonstration of cupping and capping artifacts for each dark-field CT reconstruction technique using a line profile of the images with a small blur applied. The computational phantom includes lung, bone, and soft tissue sections. The true energy-dependence of the dark-field signal is $p_0 = 3$.

Conclusions

X-ray interferometry has a wide variety of potential clinical applications, particularly in lung and breast imaging. Analogous to beam hardening in traditional CT, visibility hardening in dark-field CT can result in artifacts such as cupping, capping, or remnant attenuating structures. We have developed a new technique to account for visibility hardening in dark-field CT by incorporating a polychromatic model of the dark-field signal using a power-law distribution, producing pseudo-monochromatic dark-field images.

This technique currently relies on an assumption of the energy-dependence of the dark-field signal and known material thicknesses for attenuation-correction, but we anticipate the removal of these limitations through the inclusion of photon-counting detectors or dual-energy CT. However, the method outperforms alternative subtraction-based methods even if there is slight model mismatch.

References

[1] Meyer, H.C., Taqi, M.S., Dey, J. "Beam Hardening and Visibility Hardening Correction in Dark-Field CT", Unpublished.

[2] A. Velroyen , A. Yaroshenko, D. Hahn, A. Fehringer, A. Tapfer, M. Müller, P.B. Noël, B. Pauwels,A. Sasov, A.Ö. Yildirim, O. Eickelberg, K. Hellbach, S.D. Auweter, F.G. Meinel, M.F. Reiser, M. Bech, F. Pfeiffer, "Grating-based X-ray Dark-field Computed Tomography of Living Mice", *Ebiomedicine*, vol 2., pp. 1500-1506, 2015.

[3] Wang Z, Hauser N, Singer G, Trippel M, Kubik-Huch RA, Schneider CW, Stampanoni M, "Non-invasive classification of micro-calcifications with Phase-Contrast X-ray Mammography", *Nature Communications* vol. 5, no. 3797, May 2014

[4] Grandl, S., Scherer, K. et al. Improved visualization of breast cancer features in multifocal carcinoma using phase-contrast and dark-field mammography – an ex-vivo study. *Eur. Radiol.* **25**, 3659–68 (2015)

[5] Boone, John M. and Seibert, J. Anthony. "An accurate method for computer-generating tungsten anode x-ray spectra from 30 to 140 kV". In: Medical Physics 24.11 (1997), pp. 1661–1670. doi: https://doi.org/10.1118/1.597953. eprint: https://aapm.onlinelibrary.wiley.com/doi/pdf/10.1118/1.597953. url: https://aapm.onlinelibrary.wiley.com/doi/abs/10.1118/1.597953.

[6] Oncology Medical Physics. "CT Artifacts". Accessed: 07/15/2026. url: https://oncologymedicalphysics.com/ct-artifacts/

[7] Taphorn, Kirsten, Mechlem, Korbinian, Sellerer, Thorsten, et al. "Direct Differentiation of Pathological Changes in the Human Lung Parenchyma With Grating-Based Spectral X-ray Dark-Field Radiography". In: IEEE Transactions on Medical Imaging 40.6 (2021), pp. 1568–1578. doi: 10.1109/TMI.2021.3061253.

[8] Urban, T., Gassert, F.T., Frank, M. et al. Dark-field chest radiography signal characteristics in inspiration and expiration in healthy and emphysematous subjects. Eur Radiol Exp 9, 40 (2025). https://doi.org/10.1186/s41747-025-00578-x

Acknowledgements

This work was funded in part by NIH NIBIB Trail-blazer Award 1-R21-EB029026-01A1, the Coates Research Scholar Award, and the Charles M. Smith Superior Graduate Student Scholarship. Portions of this research were conducted with high-performance computational resources provided by Louisiana State University (http://www.hpc.lsu.edu).